Proceedings of the ASME 2017 International Mechanical Engineering Congress and Exposition
IMECE2017
November 3-9, 2017, Tampa, Florida, USA

IMECE2017-70839

EVALUATING FORCED VERSUS NATURAL CONVECTION FOR SOLAR CONCENTRATING HYBRID PHOTOVOLTAIC-THERMOELECTRIC POWER SYSTEMS MADE FROM SMALL UP-CYCLED SATELLITE DISHES

Said Alamri
Mechanical & Manufacturing Engineering Dept.
Tennessee State University
Nashville, Tennessee, USA

Turki Alamri
Mechanical & Manufacturing Engineering Dept.
Tennessee State University
Nashville, Tennessee, USA

Saud Almutairi
Mechanical & Manufacturing Engineering Dept.
Tennessee State University
Nashville, Tennessee, USA

Muhammad K. Akbar
Mechanical & Manufacturing Engineering Dept.
Tennessee State University
Nashville, Tennessee, USA

Fatemeh Hadi
Mechanical & Manufacturing Engineering Dept.
Tennessee State University
Nashville, Tennessee, USA

Matthew J. Traum
Engineer Inc
Gainesville, FL, USA

ABSTRACT

Design processes and analytical modeling are presented showing creation of a low-cost concentrating photovoltaic-thermoelectric (PV/TE) hybrid power system for research and laboratory teaching built using a small upcycled satellite dish. Today, concentrated solar hybrid PV/TE systems are drawing significant research attention and funding investment. However, the literature lacks examples of how this cutting-edge energy technology can be made accessible at low cost for STEAEM education at universities, vocational institutions, and high schools. By applying Energy Engineering Laboratory Module (*EELM*™) design principles and pedagogy, a process is presented to make this technology easily accessible at low cost.

The concentrating solar hybrid PV/TE system presented here is divided into four subsystems: 1) a concentrator, 2) a PV/TE generator, 3) data acquisition, and 4) a cooling system. The key engineering decisions governing the design for each sub-system are described. In addition, a thermodynamic analysis is presented to predict the on-sun steady-state temperature profile of the PV/TE generator at the focus of the concentrator and to determine how much electrical power it will produce.

The concentrator used is a salvaged miniature satellite dish, which is coated with mirrored tape to reflect sunlight upon a focal point. Scavenged at no cost, the satellite dish is a sectioned paraboloid of rotation offset from the vertex and the axis of symmetry. However, which paraboloid section the dish represents is unknown. A technique is presented to find the focal point and to use this information to correctly position a shadow-casting gnomon to ensure proper on-sun alignment. A method to experimentally confirm the focal location and size the PV is also provided.

A key research question for solar concentrating hybrid PV/TE power systems at this size scale is whether it is better to actively cool the TE cold side via forced convection or simply allow cooling via natural convection. The thermodynamic heat balance analysis presented to address this question finds that while forced convection does better cool the PV module, increasing its efficiency and power output, the parasitic energy expenditure of the cooling fan far exceeds the additional power produced. It is therefore more beneficial to rely on natural convection on the TE cold side to maximize power production of the overall PV/TE module.

Two experimental apparatuses were built consisting of a PV module backed by TE generators and instrumented with thermocouples to determine the internal temperature gradient while multi-meters read steady-state PV and TE power output. A halogen lamp placed at various distances from this array approximates concentrated sunlight, which is measured via pyranometer. These experiments validate conclusions drawn from the theoretical model.

INTRODUCTION

Small (less than 90-cm-diamater) discarded satellite receiver dishes have been available since 1996 when television networks began broadcasting medium-power signals from satellites [1]. Many, like the one shown in Figure 1, have been upcycled by hobbyists [2], high school science teachers, and even universities [3] into demonstration scale solar-energy-concentrating devices for Science Technology Entrepreneurship, Arts, Engineering, and Math (STEAEM) education. These systems are also used for research and even modest power generation applications. This paper presents a new approach to upcycling old satellite dishes into concentrated solar power systems. Recognizing the recent surge of interest in and funding for concentrated photovoltaic (PV) / thermoelectric (TE) hybrid power systems, this paper reports for the first time (to our knowledge) the creation of a solar concentrating PV-TE hybrid system built from a discarded small television satellite dish.

Figure 1: Discarded miniature satelight television reception dishes can be upcycled to anchor small solar concentrating hybrid PV/TE systems.

In addition to reporting this interesting and engaging educational project for engineering students, this paper addresses an important research question. At this scale, what is the best thermal regulation approach for a combined PV/TE system under concentrated sunlight to maximize output power?

At the scale of ~90 cm collector, previous researchers have suggested burying into the ground a protruding conductive fin that uses the ground as a heat sink [4]. Instead of conducting waste heat to the ground, the solution proposed and explored here is to use the heat drawn away from the PV to drive a TE bottoming cycle. Waste heat conducted through thermoelectric generators attached to the back of the PV array produce extra electrical power, which can be used for two purposes: 1) to supplement the power produced by the PV cells and 2) to provide power to drive fans imposing forced convection on the TE cold side.

BACKGROUND

Solar power production generates electricity with a limited impact on the environment as compared to other forms of electricity production. Moreover, sunlight is globally ubiquitous, making it accessible and useful nearly everywhere in contrast to fossil energy resources, which are geographically concentrated. With respect to the world's sustainable energy future, TE devices made of materials (typically ceramics) which directly convert thermal energy to electrical energy will have an important role, both as cooling and energy generation devices. Of particular interest are solar TE energy conversion systems, which convert sunlight directly into electricity with no moving parts. Xia et al. [5] reviewed the state-of-the-art with respect to this class of energy converters. Thermodynamically, TE energy converters can be thought of as solid-state heat engines, extracting useful work as heat moves down a temperature gradient from an external surface maintained at higher temperature to another external surface maintained at lower temperature. Solar TE energy converters rely on the sun to maintain their high-temperature thermal reservoir at adequate temperature and can be generally classified into three categories: 1) conventional systems, 2) hybrid systems, and 3) concentrator systems.

Conventional solar TE systems capture sunlight without any attempt to concentrate or focus it and without the addition of topping systems like heat engines or PV cells. A successful demonstration of this approach, the thermoelectric roof solar collector concept (TE-RSC), was proposed and demonstrated by Maneewan et al. [6]. TE-RSC is a residential-roof-integrated system meant for hot and humid environments. TE energy converters collect ambient sunlight to power fans within the building's roof that enhance air circulation inside the attic space while simultaneously providing convective cooling to remove heat from the cold side of the roof-integrated TE converters. This configuration, using energy produced from TE to cool the TE cold end, inspired the PV/TE hybrid configuration reported in this paper where an electric fan was considered to cool the TE cold side to increase PV efficiency.

Hybrid solar TE systems synthesize the energy conversion elements of both PV cells and TE converters. The usual motivation for this synthesis is to recover as low-grade thermal energy the excess solar energy from wavelengths of sunlight that cannot be captured by the system's PV components. Examples of this technique include the work of Kraemer et al. [7], who suggested partitioning the solar spectrum into wavelengths matched to photovoltaic band gaps and using the remainder of the spectrum to heat a TE energy converter. Another approach suggested by Vorobiev et al. [8] postulates a new PV material transparent to non-absorbed solar wavelengths. This material would pass light it could not absorb to a TE energy converter situated below it.

Solar concentrator TE systems arise from the ability for concentrated sunlight to produce very high temperature at the hot side of the TE energy converter [9]. TE energy converters exhibit the heat-engine-like property of increasing thermodynamic efficiency as the temperature gradient between the hot side and the cold side increases. Moreover, system cost benefits arise by creating a large sunlight capture area using relatively inexpensive collectors like parabolic dishes. The captured energy is then concentrated onto a small solid-state energy converter. By reducing the size of the solid-state energy converter (which is typically the most expensive system component) through energy focusing, system cost is reduced. To mitigate high temperature in concentrator systems, thermoelectric materials robust against high temperature have already been successfully developed for solar thermoelectric applications [10-12].

Combinations of hybrid and concentrated solar PV/TE systems also exist, which capitalize on the benefits of each solid-state generator type [13]. Variations on the hybrid/concentrated solar PV/TE system include the approach of physically stacking the PV and TE [7] and splitting the solar spectrum to wavelengths matched for separated PV and TE generators [14].

The recent proliferation of research interest and funding for hybrid and concentrated solar hybrid PV/TE systems [15,16] motivates need to incorporate into undergraduate engineering, vocational, and even high school STEAEM curricula relevant hands-on laboratory and training experiences. While modern experimental concentrated solar PV/TE systems are complex and expensive, analogous teaching systems that convey essential skills and understanding need not be. One goal of this paper, therefore, is to describe the design methodology and analysis used to develop an inexpensive concentrated solar hybrid PV/TE system for research and teaching.

EDUCATIONAL MOTIVATION

Lack of energy-related knowledge among American students and the general public is endemic according to DeWaters and Powers [17] and to Condoor [18]. As the world transitions toward a renewable energy future, familiarity with energy and sustainability concepts will become increasingly important. Increasing green-energy-focused education is essential to meet the growing demand for sustainability-conscious technical professionals, and curriculum contents must stay relevant in addressing the current state of the art.

With respect to integrating emerging energy technologies into curricula, one solution is to create a broadly-accessible introductory-level elective course in energy engineering. UC Santa Cruz, for example, created "Renewable Energy Sources," a prerequisite-free class that attracts students from all STEAEM fields as well as humanities and social sciences [19]. The course is built around seven simple renewable energy experiments including a flywheel; sun tracker; fuel cell; and power conversion through photovoltaic, hydroelectric, thermoelectric systems. While laudable both for its ubiquitous and accessible student engagement and its seamless insertion of hands-on energy activities into STEAEM and general curricula, the UC Santa Cruz approach requires a whole new class to be created along with an associated curriculum adjustment for programs wishing their students to take "Renewable Energy Sources".

As an alternative to creating a new class, the "Energy Engineering Laboratory Module" (*EELM*™) approach can be pursued. This approach posits that energy is a topic ubiquitous to all STEAEM fields, and therefore hands-on laboratory and training experiences can be developed for ubiquitous and seamless insertion into any STEAEM course, especially at the advanced high school and college levels. Detailed description and examples of successful implementation of the *EELM*™ pedagogy have been published elsewhere [20-23]. By their nature *EELM*™ laboratories are hands-on, accessible, economical, and "turn-key". The hardware must be affordable for an institution with limited resources; provide students with meaningful, open-ended, hands-on learning experiences; and can be built and operated by a handy course instructor or technician without situated knowledge or access to specialized tools and equipment.

Design and analysis processes used in this paper to create a concentrating solar hybrid PV/TE system were developed by an undergraduate mechanical engineering Capstone senior design team following *EELM*™ pedagogy. The team acquired the satellite dish from a previous Capstone team that built a simple parabolic solar concentrator with mirrored surface to focus collected sunlight to boil water. The current solar concentrating hybrid PV/TE project reported here builds on that existing apparatus by adding a target with embedded solid-state power generator with stacked PV and TE generators to convert captured, concentrated sunlight to electrical power.

DESIGN PROCESS

To facilitate design, the overall system was divided into four subsystems: 1) Solar Concentrator, 2) PV-TE Generator, 3) Data Acquisition, and 4) Cooling System. Each sub-system was developed individually, and they were then combined together into a working prototype. Following the formal engineering design process [24], numerous solutions for each sub-system were brainstormed. A benchmark solution was then identified for each subsystem and prototyped.

Solar Concentrator Subsystem

The parabolic solar concentrator subsystem was created using a scavenged miniature parabolic television satellite dish. The dish was positioned on a two-axis mount that can rotate 360 degrees about the Z-axis and rotate up and down 180 degrees about the X-axis, allowing manual sun tracking at any location in the sky. While automated solar tracking is possible with this setup and will be implemented in a future Capstone design project, that capability was deemed less important than maximizing power generation for this phase of the project.

The solar concentrator is a sectioned parabola of rotation offset from the vertex and the axis of symmetry as shown in Figure 2. Any ray of sunlight entering normal to the

paraboloid's virtual aperture will reflect from the mirrored surface and be concentrated at a single focal point. This focal location is where the PV/TE generator must be placed to intersect maximum concentrated sunlight.

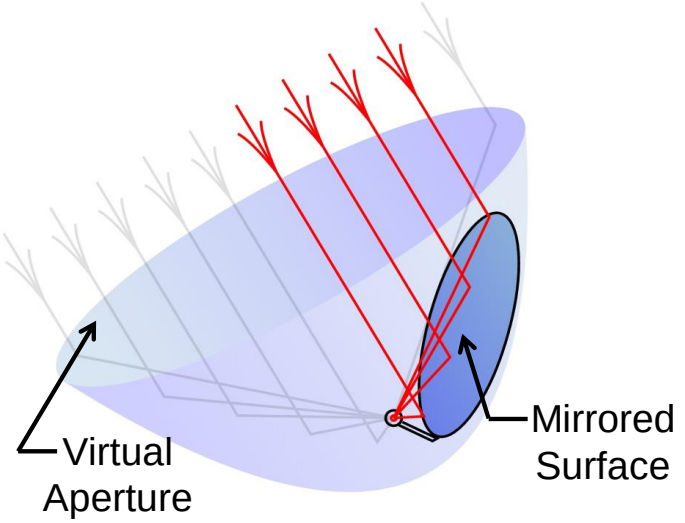

Figure 2: Dark blue represents the solar collector television satellite dish. It is a section of a larger parabola of rotation (light blue) and offset from the vertex and the axis of symmetry. Sunlight rays entering normal at the parabola's virtual aperture are focused to a point by the dish.

A method is needed both to locate the focal point for an arbitrary parabolic section and to determine the angle between the virtual aperture and the actual aperture so the dish can be correctly focused on the sun. This angle provides the orientation for a gnomon, which is used to manually point the collector toward the sun in the orientation that maximizes sunlight reflection onto the focal point. The focal point location was determined theoretically based on geometric analysis, and this location was then verified experimentally as described in detail elsewhere [25].

The method developed requires measurement of only three physical dish dimensions (Figure 3): its 1) height, 2) width, and 3) depth. The focal length, F, is then located using the following geometric equation,

$$F = \frac{W^3}{16DH} \tag{1}$$

As shown in Figure 3, a foil-tape-covered mirror affixed to the satellite dish is used to reflect sunlight onto the focal point. The foil tape does not require any glue, i.e., it is sticky and flexible. While various reflector materials are available, a previous group of Capstone students experimented with different reflectors and found that the foil mirror is the best choice. The comparison reflectors experimented with were 1) small pieces of mirror, 2) aluminum foil, and 3) white paint. The theoretical reflectivity of the foil mirror used in this project is 97%, and the experimentally measured reflectivity is 87%.

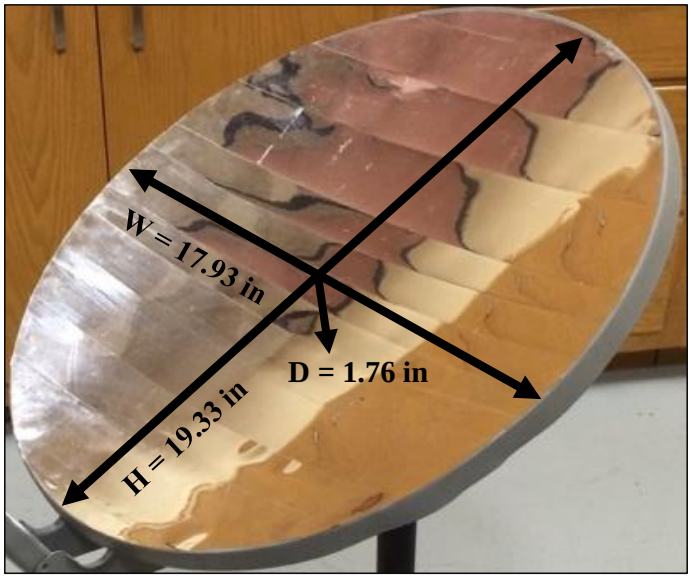

Figure 3: Measurements of the sectioned satellite dish used as a solar concentrator enable focal point location and gnonon angle calculation for correct on-sun orientation.

The focal point location can also be determined experimentally by holding a target in the focal plane and traversing it until the concentrated sunlight spot is brightest, as shown in Figure 4. Importantly, it is uncertain which parabolic section the collector represents (see Figure 2) since it was scavenged from a past project, and no manufacturer information is available. As the section is offset and focusing on the sun is a manual process, a gnomon is needed to orient and focus the collector. It must point normal to the virtual aperture of the parabola to ensure the sun's rays enter normal to that plane. Pointing the gnomon normal to the actual aperture of the parabolic section embodied by the satellite dish does not provide correct focus. The correct gnomon angle with respect to the actual dish aperture is given by the following equation.

$$\cos \Theta = W/H \tag{2}$$

Using the measured dish dimensions shown in Figure 3, it was determined that the gnomon for the dish used here must be offset 23° from normal to the real aperture of the mirrored satellite dish to achieve proper focus.

Solid State Generator Subsystem

Commercial PV and TE panels were purchased and combined into a generator. The PV panel was purchased from Adafruit and was manufactured by Voltaic Systems. The module is 210 mm X 113 mm X 5 mm, waterproof, scratch resistant, and UV resistant. The panel contains high efficiency monocrystalline cells with a total rated output of 3.5 Watts at 6 volts and is mounted on a plastic-aluminum composite ($k_{pv} \approx$ 0.25 W/m-K). This module was selected as it is slightly larger than the experimentally-determined size of the concentrator's focal spot (Figure 4). Thus, all photons reflected from the parabolic dish are intersected by the PV module when it is

located at the focal point, providing the opportunity for maximum photon absorption and electrical power production or thermal heat transfer to the TE generator.

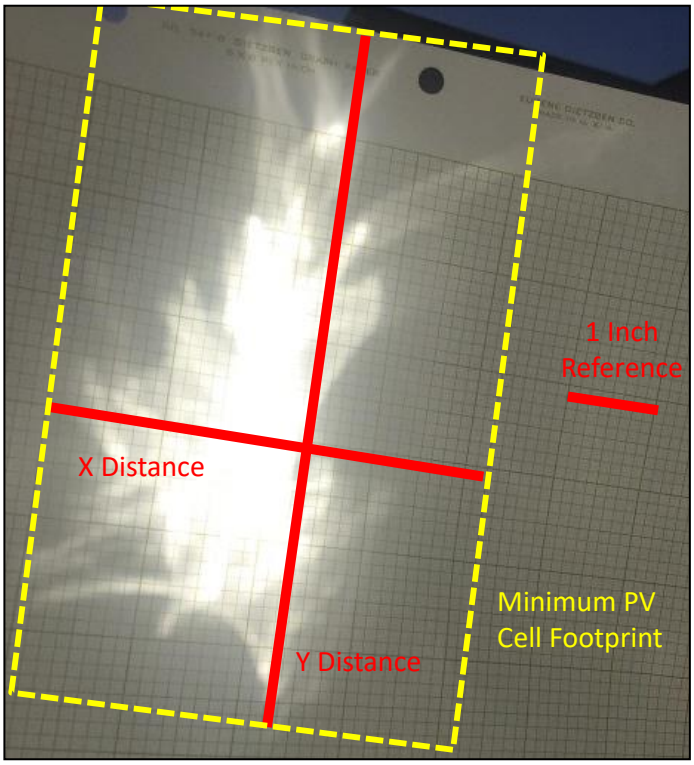

Figure 4: Measurement of the focal area by digital photography on graph paper reveals a wide 'smear' of concentrated energy instead of a confined focal point.

As commercially available TE generators are generally smaller than the purchased PV module, two different types of TE generators were mixed to most closely match the PV module area. The larger TE generators are part number TEC1-12730 from Hebei I.T. (Shanghai) Co., Ltd. These modules are 62 mm X 62 mm X 3.9 mm capable of producing 282 Watts under a 79 K temperature gradient. The smaller TE generators come from Adafruit and are 40 mm X 40 mm X 3.5 mm. These modules can produce 97 Watts at 15.3 volts.

As shown in Figure 5, these TE generators were tiled on the back of the PV module to maximize coverage area. The PV module has four mounting screws at its corners. A thin steel plate was used to hold the TE's in place by synching it down on these mounting screws. ARCTIC MX-4 carbon-based heat sink compound thermal paste was used between the PV and TE's as well as the TE's and the steel plate to reduce contact resistance.

Data Acquisition Subsystem

To understand its function, various voltages, currents, and temperatures need to be measured and logged while the system is operating. Data acquisition is accomplished using a Raspberry Pi 3 micro-computer coded in the Python programming language. The power required to run this data acquisition system is not included in the parasitic energy budget of the overall system. This choice is justified because even through it is instructive to see various experimental data streams to validate theoretical analysis, if the system were a commercial power-producing product, extensive data acquisition would likely not be required.

Figure 5: Two sizes of TE generator are tiled on the back of the PV module to maximize area coverage. The key in the picure provides a sense of scale for the PV-TE target assembly.

Cooler Subsystem

In the hybrid PV/TE configuration, the TE serves two functions. First, it creates excess electricity from waste heat generated by sunlight absorbed by the PV (but not directly converted into electricity). Second, it provides a heat transfer conduit between the PV and a cooling system that keeps the PV at low temperature to improve power generation.

Without cooling, PV cells under concentrated sunlight become less efficient due to high operating temperature [26]. Thus, utility-scale PV power installations often use water as a coolant to maintain efficiency. Air-cooled condensers could reduce the amount of water required for large scale solar projects, but this approach is less efficient than direct-water-cooled methods.

While liquid water cooling received the highest Pugh Chart score from the student design team, active liquid cooling loops negate two major incentives for using solid-state generators for solar energy conversion: 1) eliminating potential fluid leakage of a conventional heat engine and 2) eliminating moving parts. One method to use liquid cooling for the concentrating solar hybrid PV/TE system while eliminating pumps was considered based on the siphon-driven system of Furushima and Nawata [27]. However, in this configuration municipal water pressure provided potential energy to initiate and maintain the siphon. Thus, a siphon-based solar concentrating PV/TE system could not operate in remote areas away from a pumped municipal water supply. It is these remote locations where the technology (when scaled up to utility scale) is most desirable and competitive. So, liquid cooling loops were eliminated from consideration.

Forced convection and natural convection of ambient air over a large surface well-connected thermally to the TE cold end received the second and third highest Pugh Chart scores

respectively from the student design team. Thus, analytical models for each approach were developed and analyzed to determine the solution that provides the highest overall system power output.

THEORETICAL MODELING

To predict performance of the solar concentrating hybrid PV/TE system, a thermodynamic energy balance model, shown schematically in Figure 6, was developed with the goal of evaluating total power output in response to two different convection boundary conditions on the TE cold side: natural convection and forced convection.

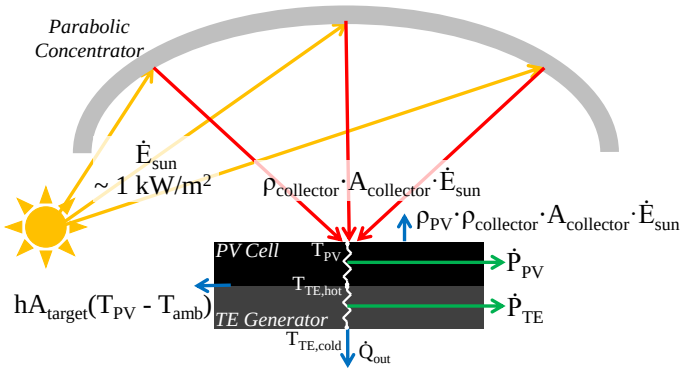

Figure 6: The one-dimensional energy balance model schematic for the solar-concentrating hybrid PV/TE system.

The forced convection model includes an empirical relationship for the air velocity produced by a small RC drone fan as a function of fan input power. A small fan of this type was considered to force air over the TE cold side in the generator assembly. In a supporting experiment, a drone fan was instrumented to determine its power consumption, and it was fitted with a pitot-static probe attached to a Dwyer Mark II 25 manometer to determine flow velocity as a function of input power. Measured flow velocity as a function of input power was then used to estimate the forced convective heat transfer coefficient over the TE cold end based on order-of-magnitude ranges provided by Mills [28].

While adding forced convection will draw electrical power away from the system to drive the fan, it is possible that supplemental cooling by the fan will increase the PV efficiency, more than offsetting the power required to drive the fan. To generate reasonable flow velocity inducing a forced convection coefficient significantly larger than that of natural convection, the fan used here must draw at least 6.72 watts.

The model assumes that the system is in steady state, all components are homogenous, conduction is one-dimensional, and there is no contact resistance between components. The cross-sectional area of the PV/TE target module, A_{target}, is assumed to be uniform throughout the module even though the TE generators are smaller than the PV module and are therefore tiled on the back as shown in Figure 5. The schematic of Figure 6 shows the energy flow through the system and the 1-D resistor model used for energy balance analysis. Table 1 lists the constant parameters used in the model to represent the solid-state generator subsystem. The values for natural and forced convection coefficient ($h_{natural}$ = 10 W/m^2-K and h_{forced} = 100 W/m^2-K respectively) are in the middle of the ranges for those heat transfer modes suggested by Mills [28]. As these coefficients are weak functions of temperature in the ranges studied, no attempt is made to calculate more precise values. Future modeling improvement will include more explicit calculations of these coefficients.

Table 1: Parameters used in analytical model.

Parameter	Value	Units
$A_{collector}$	0.18	m^2
A_{target}	0.02373	m^2
$\dot{E}$	1000	W/m^2
k_{PV}	0.25	W/m-K
K_{TE}	2.6	W/K
h_{PV}	10	W/m^2-K
h_{TE}	100	W/m^2-K
L_{PV}	0.005	m
L_{TE}	0.0039	m
T_{amb}	297.2	K
$T_{pv,ref}$	298	K
Z	0.0026	1/K
α	11	%
β	-0.0045	%
$\rho_{collector}$	0.87	N/A
ρ_{PV}	0.6	N/A

In considering the overall system energy balance, first sunlight enters from the surroundings and strikes the collector. Some portion reflects and focuses onto the face of the PV module. Some portion is absorbed by the PV directly producing electricity. Some is absorbed as heat. The remainder is reflected away from the PV module face. Energy absorbed by the PV module (both to produce electricity and to conduct through as heat) is encompassed by the first term on the left side of the energy balance equation.

$$(1-\rho_{PV})\rho_{collector}A_{collector}\dot{E}_{sun} = h_{PV}A_{collector}(T_{PV}-T_{amb}) + h_{TE}A_{collector}(T_{TE,cold}-T_{amb}) + \dot{P}_{PV} + \dot{P}_{TE} \quad (3)$$

The right-hand side of Eq. 3 accounts for heat lost from the PV surface via natural convection, heat lost from the TE cold surface via natural or forced convection, and electrical power produced by the PV and TE modules.

Also important is the rate of heat transfer through the PV cell or module into the TE generator. The greater this heat transfer, the more thermal power is available for the TE to convert to electrical power. Since PV cells are very thin and thermally conductive compared to the protective modules typically encasing them, the PV cell thermal resistance is ignored when modeling a system where an encased cell is used. In its place, the thickness (L_{pv} = 0.005 m) and thermal conductivity of the thermoplastic casing (k_{pv} ≈ 0.25 W/m-K) are used. When modeling a system where the PV cell is bare and unenclosed, the cell thickness (L_{pv} = 0.00023 m) and thermal conductivity of polycrystalline silicon (k_{pv} ≈ 150 W/m-K) [29] are directly used.

To determine the power produced by TE modules, the temperature-dependent energy conversion efficiency of a TE generator, η_{TE}, must be evaluated. The relationship depends on three parameters [30]: the hot side temperature, $T_{TE,hot}$; the cold side temperature, $T_{TE,cold}$; and the thermoelectric figure of merit, Z.

$$\eta_{TE} = \frac{(T_{TE,hot} - T_{TE,cold})}{T_{TE,hot}} \frac{\sqrt{1+Z\left(\frac{T_{TE,hot}+T_{TE,cold}}{2}\right)}-1}{=\sqrt{1+Z\left(\frac{T_{TE,hot}+T_{TE,cold}}{2}\right)}+\frac{T_{TE,cold}}{T_{TE,hot}}} \quad (4)$$

The TE temperature terms in the efficiency expression are determined by the PV/TE internal temperature gradient arising from the 1-D heat transfer model. To determine TE figure of merit, Z, the method of Luo [31] is used based upon the manufacture's data sheet at conditions of $T_{TE,hot}$ = 50 °C [32]. This estimate gives Z = 0.0027 1/K as well as module thermal conductance, K_{TE} = 2.60 W/K. To check temperature stability, these values were rechecked based on datasheet conditions at $T_{TE,hot}$ = 25 °C. The resulting Z = 0.0026 1/K and K = 2.7 W/K represent a 3.1% and 4.0% change, respectively.

It was assumed, therefore, for this analysis that Z and K_{TE} are constant and independent of temperature for the operating range evaluated. Certainly, more sophisticated models to approximate TE performance under variable temperatures exist [10], but the equations and analysis used here are adequate for the goal of determining whether free or forced convection over the TE cold face is preferred. Thus, the equation for TE power generation is the product of TE efficiency and the rate of thermal power entering the TE. This thermal power rate is the rate of heat conduction through the PV into the TE.

$$\dot{P}_{TE} = \eta_{TE}\dot{Q}_{PV,out} = \eta_{TE}\frac{k_{PV}A_{target}}{L_{PV}}\left(T_{PV} - T_{TE,hot}\right) \quad (5)$$

For power produced by the PV module, a widely-applied temperature-dependent linear energy conversion efficiency model is used. This model is dependent upon one variable parameter, the PV cell temperature (T_{PV}), and two empirical parameters, the reference cell efficiency, α, and the reference cell temperature coefficient, β [26,33,34].

$$\eta_{PV} = \alpha\left[1 + \beta\left(T_{PV} - T_{PV,ref}\right)\right] \quad (6)$$

The linear relationship between PV cell temperature and efficiency was experimentally verified for concentrated PV by Kemmoku et al. [35] Field deployed flat plate single crystalline silicon PV modules have a maximum measured efficiency not exceeding 12% (at $T_{PV,ref}$ = 300 K) [36]. The reference cell temperature coefficient for silicon PV is between -0.003 %/K and -0.006 %/K (at $T_{PV,ref}$ = 300 K) [37]. It is therefore assumed in this model that α = 0.11 and β = -0.0045 %/K and that these parameters are not functions of temperature. Thus, the equations for PV power generation is the following.

$$\dot{P}_{PV} = \eta_{PV}(1-\rho_{PV})\rho_{collector}A_{collector}\dot{E}_{sun} \quad (7)$$

$$\dot{P}_{PV} = \left\{\alpha\left[1 + \beta\left(T_{PV} - T_{PV,ref}\right)\right]\right\} \times \left[(1-\rho_{PV})\rho_{collector}A_{collector}\dot{E}_{sun}\right] \quad (8)$$

EXPERIMENTAL MEASUREMENTS

Two experiments were created in attempts to validate the 1-D energy balance model. The first experiment used the PV module backed by TE generators taken directly from the concentrator apparatus described above in the "*Solid State Generator Subsystem*" subsection. As will be detailed later, this first experiment had several problems. It was not able to tolerate solar flux exceeding 1000 W/m^2 without component failure. It was both electrically and thermally complex owing to the multiple TE generators used (see Figure 5), creating doubts about whether the generators were operating at their Maximum Power Point (MPP) and whether a 1-D resistance model adequately represents the system's internal temperature profile.

Ultimately, a second experiment was created to mitigate issues encountered when testing the first apparatus. The second unit was specifically designed to tolerate high temperature and high solar flux consistent with concentrated sunlight. It used a single, un-encapsulated PV cell mounted to a single TE generator that both drove loads consistent with their measured MPP's. Finally, the second experiment was smaller in size than the first to promote development of an internal temperature profile as amenable as possible to one-dimensional heat transfer.

Experiment #1: Based on the Solid-State Generator Subsystem

For the first experiment, the hybrid PV/TE module was taken directly from the solar concentrator apparatus (see Figure 7) and instrumented with four thermocouples, which are read simultaneously by two Leaton® digital dual-channel thermocouple thermometers. The thermocouples were bare bead K-Types and were fixed in place using the high-thermal-conductivity epoxy method described by Traum [38], which is known to produce high-quality contact surface temperature measurements. The thermocouples were strategically placed on and in the hybrid PV/TE module at locations corresponding to where temperatures are calculated in the analytical model. One thermocouple is placed on the sun-exposed PV module surface directly in the center. The second is placed on the sun-exposed PV module surface in the top right corner; comparing these two measurements enables determination of whether the 1-D heat transfer assumption underpinning the model is correct. The third thermocouple is placed on the backside center of the PV module where it interfaces the central 62 mm X 62 mm TE generator. This location simultaneously enables quantification of the heat transfer through the PV module as well as the hot side TE temperature. The forth thermocouple is located on the back side of the TE directly across the generator from the third thermocouple; its purpose is to measure the TE cold side temperature. Since the mounting holding the TE's to the PV module is 1/16-inch-thick steel plate, the temperature gradient

it supports along its thickness is below the resolution of a thermocouple. So, it was decided not to place a redundant thermocouple on that plate. To mitigate thermocouple fin effect, the wires were directed internally within the PV/TE module and allowed to run its length to reduce parasitic heat transfer to ambient.

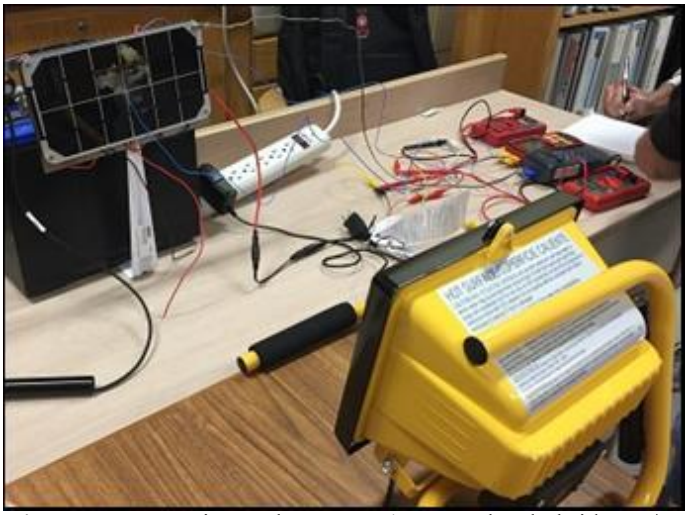

Figure 7: Experimental setup #1 uses the hybrid PV/TE module taken directly from the solar concentrator apparatus to measure its internal temperature profile and the resulting power produced under halogen lamp illumination in lieu of concentrated sunlight.

The module's TE generators were wired in series so their cumulative voltages would be additive. Both the PV and TE generators were then wired across individual 1000 Ω resistors to provide load. Voltage and current produced were measured simultaneously using CenTech 98025 digital multi-meters set in voltmeter and ammeter mode respectively. Photon flux on the exposed PV module face was measured using an Apogee Instruments silicon-cell SP-214 pyranometer mounted in the plane of the PV module.

Initially, the experiment was attempted on-sun with the hybrid PV/TE generator mounted in the focus of the concentrating parabolic dish. However, the plastic component of the module encasing the PV cells began to melt during tests. It was later realized that the module's thermoset plastic had a melting temperate of ~130 °C while early tests showed the PV face would reach at least 165 °C. In Experiment #2, a bare polycrystalline PV cell without a thermoplastic mount is used to avoid module melting under high photon flux.

To test the hardware as-built, the experiment was run under illumination from an Ironton 500-Watt, 8000-Lumen Halogen work-light (see Figure 7), which provides illumination similar to the sun without producing excessive temperature and inducing melting on the PV module mount surface. To change photon flux on the PV surface, the distance between the hybrid PV/TE module and the lamp was increased between experimental runs corresponding to a drop in illumination flux registered on the pyranometer.

With the distance between the lamp and PV surface set to produce desired illumination flux, the lamp was turned on, and the thermocouple transients were monitored until the whole system was in steady state. This process usually took about 5 minutes per experiment. Once steady-state conditions were achieved, data for that condition were taken by-hand from all instruments. Four experiments were run with the only independent variable parameter being illumination flux, which was increased each time by moving the halogen lamp closer to the hybrid PV/TE apparatus to obtain the following values: 383 W/m^2, 465 W/m^2, 773 W/m^2, and 1081 W/m^2.

Experiment #2: Purpose-Built to Validate the Thermal Model

The second experiment, shown in Figure 8, was purpose-built to mitigate experimental and measurement issues encountered when testing the first experiment, which was taken directly from the solar concentrator apparatus and not designed for testing in the lab.

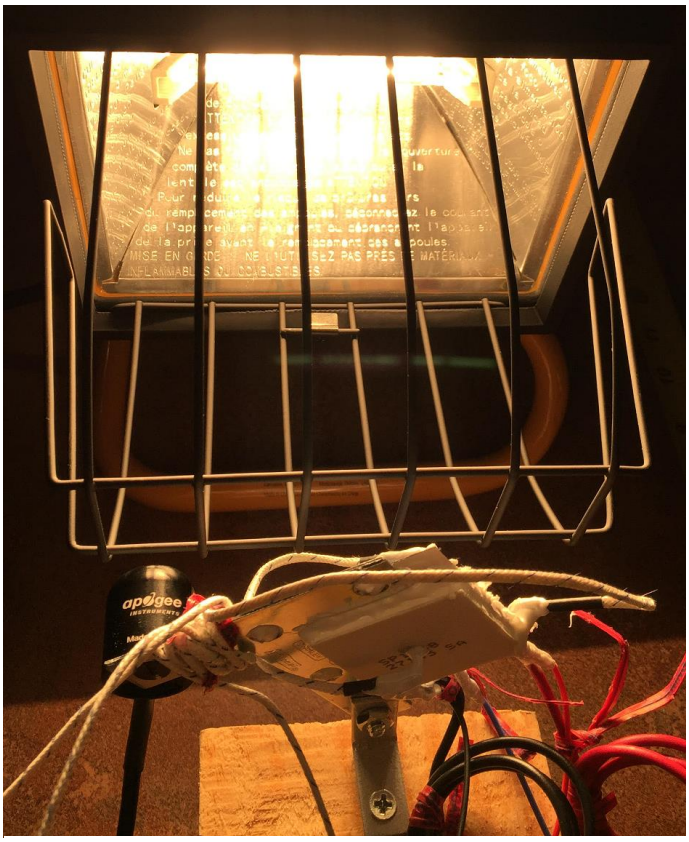

Figure 8: Experiment #2, purpose-built for laboratory evaluation, is shown under halogen lamp illumination. It was designed to tolerate much higher illumination flux than the first experiment would withstand while providing easier measurement of the internal temperature profile and power produced by the PV and TE generators.

Need for the second experiment informed an important pedagogical lesson for the student Capstone design team. Since the hybrid PV/TE target of Experiment #1 was initially

designed to maximize on-sun photon capture from the parabolic dish concentrator, it was not meant for evaluation in the laboratory, and it proved difficult to evaluate. Ultimately, a second experiment designed specifically for laboratory evaluation was needed. Instructors wishing to replicate the experimental analysis portions of this project should consider building two experiments optimized accordingly: one for field demonstration and the second instrumented for laboratory interrogation.

Experiment #2 was built using a single bare Aoshike 52 mm X 52 mm polycrystalline silicon solar cell rated for 0.46 watts at 0.5 volts. Unlike the PV array of Experiment 1, this cell was not encased inside a thermoplastic module and could therefore operate at much higher temperature before component failure. The PV cell was backed with a Laqiya 40 mm X 40 mm high temperature Peltier TE generator rated for operation at 150°C. As shown in the construction image of Figure 9, the PV and TE were held together using OMEGABOND® 101 high thermal conductivity two-part epoxy applied around the TE edges with ARCTIC MX-4 thermal carbon-based heatsink paste sandwiched between to reduce contact resistance. A thermocouple was epoxied to the back of the PV and sandwiched between the PV and TE in the thermal paste to measure temperature at that interface. This internal module temperature measurement capability was not ultimately available in Experiment #1 as that thermocouple broke off.

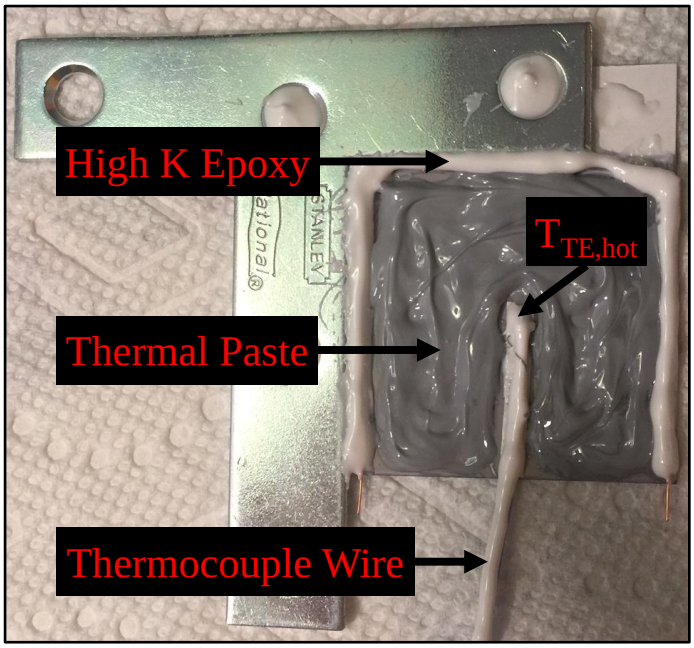

Figure 9: Experiment #2 is shown in mid-construction to reveal how the PV and TE modules are attached together and how the internal temperature at the PV/TE interface is measured. This image also shows the "thermal horn", a metal 'T' fixed with epoxy to the back of the bare PV cell to support it, provide a thermal anchor for thermocouple wires, and platform-mount the experiment.

As shown in Figure 10, the apparatus includes three additional thermocouples: the TE cold side, the front face edge of the PV, and the center of the PV. While thermocouples fixed to the front of the PV do slightly shade this generator, the affected area is small and assumed not to impact PV performance. All thermocouples used in Experiment #2 are bare-bead K-Types manufactured by Uxcell. The four thermocouples are read simultaneously by two Leaton® digital dual-channel thermocouple thermometers.

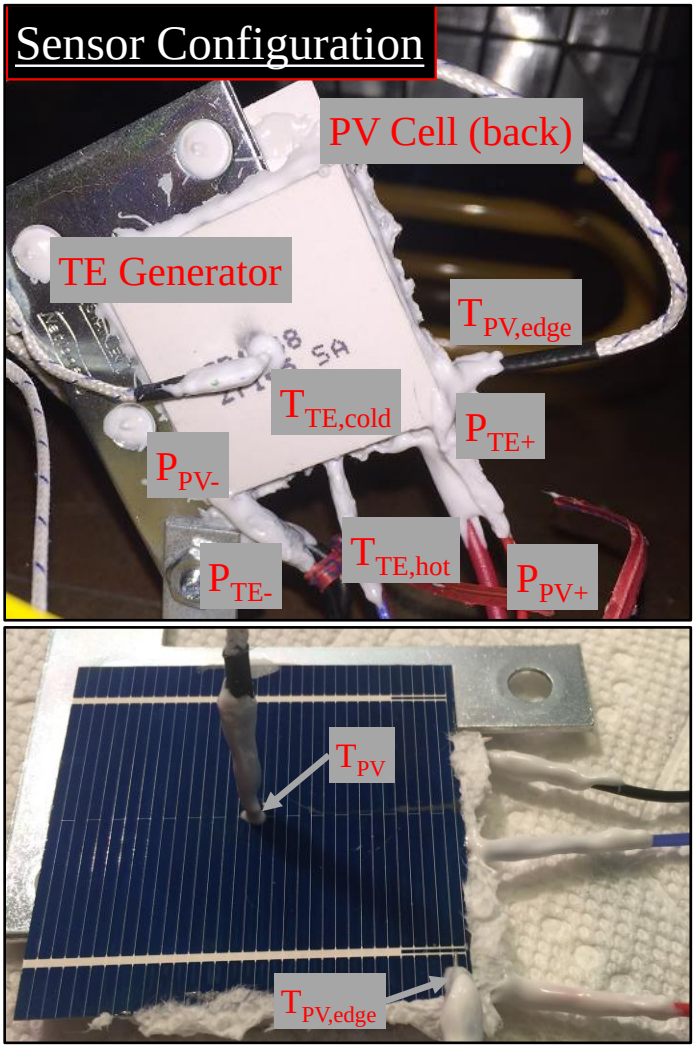

Figure 10: (TOP) The back side of the Experiment #2 hybrid PV/TE generator shows how the apparatus is instrumented with thermocouples and power wires. (BOTTOM) A pair of thermocouples is attached to the PV face of the apparatus with epoxy to measure the temperature of this surface and evaluate validity of the one-dimensional internal temperature profile assumption underpinning the thermal model.

To prevent electrical cross-talk between the two PV-face-mounted thermocouples, a thin thermally-conductive and electrically-resistive adhesive was placed under the edge-mounted thermocouple before it was epoxied in place. To

negate thermocouple fin effect, all thermocouples were wrapped around a metallic "thermal horn" (Figure 9) that was used both to support the PV cell and mount the entire experiment to its stand. Due to its placement on the back of the PV, the thermal horn's temperature approximates that of the PV cell. Figure 10 also shows the electrical-power-carrying wires emanating from the PV and TE generators. These wires were coated in OMEGABOND® 101 epoxy to provide strain relief.

Figure 11 shows the data acquisition set-up and operational arrangement for Experiment #2. Illumination is provided by a 500-Watt Woods L20 8000-Lumen halogen work light. Illumination flux is modulated by moving the lamp with respect to a tape measure either toward or away from the apparatus. Unlike Experiment #1, which produced just over 1000 W/m^2 illumination flux and failed thermally when exposed to concentrated sunlight, Experiment #2 produced and withstood nearly 2500 W/m^2. This illumination flux level is more representative of concentrated sunlight produced by a small television-dish-based concentrator. The flux is measured using an Apogee Instruments SP-420 pyranometer mounted in the plane of the PV cell and logged via a USB-connect laptop PC running ApogeeConnect software.

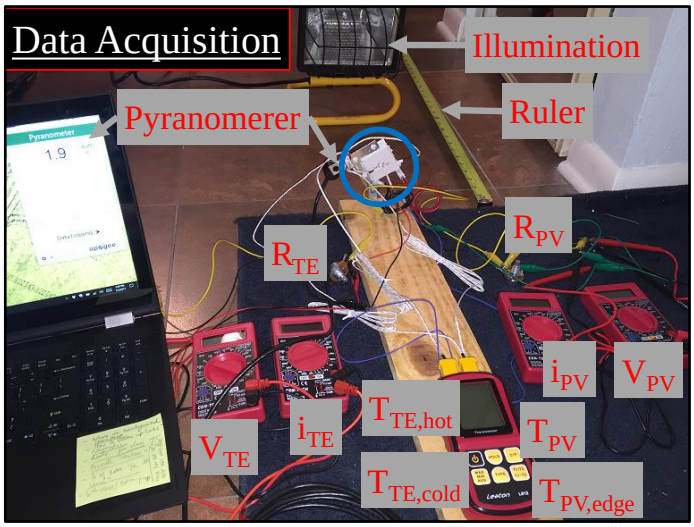

Figure 11: Data acquisition setup and instrumentation used to monitor Experiment #2.

To find their MPP's, the PV and TE generators were individually wired to variable resistors with a 0- to 25-ohm range to provide load. PV and TE voltage and current were measured simultaneously using CenTech 98025 digital multi-meters set in voltmeter and ammeter mode respectively. With the apparatus under a modest 500 W/m^2 illumination, the potentiometers were manually varied over their full resistance range, and PV and TE power produced was measured as a function of resistance to determine the MPP. The PV cell's MPP was located at 21.5 ohms, but the TE MPP was not reached when the attached variable resistor hit the top of its range, 26.8 ohms. A larger resistor was not available. The PV and TE resistors were thus fixed at 21.5 ohms and 26.8 ohms respectively for all subsequent experiments. In future experiments TE MPP will be found and set using a variable resistor with higher range. Also, since MPP is a function of operating conditions, the resistance to achieve MPP will be found for each unique solar flux condition evaluated to maximize the power output of the PV and TE for each test.

Experiments were run in a dark room to prevent the PV from absorbing ambient light and producing secondary power. With the distance between the lamp and PV surface set to produce desired illumination flux, the lamp was turned on, and the thermocouple transients were monitored until the whole system reached steady state. This process usually took about 5 minutes per experiment. Once steady-state conditions were achieved, data for that condition were taken by hand from all instruments. Three experiments were run with the only independent variable parameter being illumination flux, which was increased each time by moving the halogen lamp closer to the hybrid PV/TE apparatus to obtain the following values: 988 W/m^2, 1917 W/m^2, and 2450 W/m^2. Since the apparatus of Experiment #2 could withstand higher temperatures than the previous version, it was possible in these tests to illuminate it to 2450 W/m^2, which is just under 2.5 times the intensity of normal sunlight. This condition was intended to represent performance of the system under concentrated sunlight.

RESULTS

Results from both experiments were compared to the internal temperature profile and output power predictions from the theoretical model by adjusting appropriate model parameters to match each experiment. Although the actual experiments relied only on natural convection to cool the TE cold end, model results were generated for both natural and forced convection boundary conditions to provide insight on whether adding a fan to induce forced convection would enable either system to produce enough supplemental energy to justify the fan's addition.

Equations (3) – (8) were coded into MATLAB along with constitutive heat conduction equations arising from Figure 6. The system of equations was solved simultaneously to determine the internal temperature profile of both PV/TE generators as well as their resulting power outputs.

Results: Experiment #1 -- Based on Solid-State Generator Subsystem

Experimental and associated model results for the PV/TE module pulled directly from the on-sun experimental system are given in Table 2.

Results: Experiment #2 -- Purpose-Built to Validate the Thermal Model

Experimental and associated model results for the PV/TE module purpose-built to validate and explore the 1-D heat transfer and thermodynamic model embodied in Figure 6 are given in Table 3.

Table 2: Experimental and complementary theoretical model results from the Experiment #1 apparatus showing performance differences between natural and forced convection. Note that the TE hot side temperature (where the PV and TE generators interface) was not measured (N/M) in Experiment #1.

	Flux	Temperatures [K]				PV	TE	Total
Designation	[W/m^2]	T_{PV}	$T_{PV,edge}$	$T_{TE,hot}$	$T_{TE,cold}$	Power [mW]	Power [mW]	Power m[W]
Experiment	1081	324.1	312.1	N/M	309.4	46	0.064	46.03
Model (Nat Conv)	1081	320.0	320.0	316.6	315.0	1020	3.033	1023.03
Model (Forced Conv)	1081	309.0	309.0	303.4	300.8	1080	8.325	1088.33
Experiment	773	304.4	300.5	N/M	297.8	49	0.046	48.91
Model (Nat Conv)	773	313.5	313.5	311.1	310.0	750	1.517	751.52
Model (Forced Conv)	773	305.4	305.4	301.6	299.9	780	3.837	783.84
Experiment	465	306.0	303.2	N/M	303.4	43	0.012	43.44
Model (Nat Conv)	465	307.0	307.0	305.6	305.0	470	0.519	470.52
Model (Forced Conv)	465	301.9	301.9	299.9	299.0	480	1.064	481.06
Experiment	383	303.2	301.9	N/A	302.4	38	0.007	38.14
Model (Nat Conv)	383	305.6	305.6	304.4	303.9	390	0.369	390.37
Model (Forced Conv)	383	301.5	301.5	299.7	298.90	390	0.862	390.86

Table 3: The Experimental and complimentary theoretical model results from the Experiment #2 apparatus showing performance differences between natural and forced convection.

	Flux	Temperatures [K]				PV	TE	Total
Designation	[W/m^2]	T_{PV}	$T_{PV,edge}$	$T_{TE,hot}$	$T_{TE,cold}$	Power [mW]	Power [mW]	Power [mW]
Experiment	2450	453.2	453.2	444.2	393.2	0.000483	2.181	2.18
Model (Nat Conv)	2450	368.5	368.5	368.5	318.0	200	3.213	203.21
Model (Forced Conv)	2450	363.7	363.7	363.7	300.5	210	5.037	215.04
Experiment	1917	359.0	359.0	349.0	337.3	0.000037	1.213	1.21
Model (Nat Conv)	1917	352.7	352.7	352.7	313.0	170	1.181	171.18
Model (Forced Conv)	1917	347.9	347.9	347.9	299.9	180	2.912	182.91
Experiment	988	337.3	334.5	326.0	310.0	0.000009	0.059	0.06
Model (Nat Conv)	988	324.5	324.5	324.5	305.5	100	0.454	100.45
Model (Forced Conv)	988	324.3	324.3	324.3	299.0	100	0.098	100.10

DISCUSSION

Examining the measured temperatures at the center and the edge of the PV face for both Experiment #1 and Experiment #2, it is observed that the temperatures are very similar; usually within the measurement uncertainty of the thermocouples for most experimental runs. This trend is more prominent in the Experiment #2 apparatus, which was designed intentionally to promote a one-dimensional internal spatial temperature gradient. Temperature uniformity across the PV face improves for Experiment #2 at increased solar flux. These results indicate that the assumption of a one-dimensional internal temperature profile within the experimental apparatuses is valid, lending additional confidence to use of a simple 1-D resistor-based thermal model to predict theoretical temperatures and performance of these systems.

Comparing expected power output from the theoretical model to measured power outputs for the two experiments reveals that the model grossly over-predicts the true power output of the real systems but under-predicts the expected power output based on manufacturer data sheets. Checking manufacturer specifications, the Voltaic Systems PV module used in Experiment #1 should produce 3.5 Watts under normal sunlight, which is comparable in order of magnitude terms to 1.02 watts, the Experiment #1 model power output result for 1081 W/m^2 illumination flux. The actual measured PV power output under this test condition was only 0.046 watts (see Table 2); much lower than expected.

While this mismatch might be explained for the apparatus of Experiment #1 owing to thermal damage it sustained when exposed to concentrated sunlight, model/experiment results disagreement cannot be easily explained for Experiment #2. In these experiments, the PV cell was electrically loaded correctly and operating at its MPP, and yet the resulting power it produced was so miniscule as to be almost undetectable. Reviewing the specifications from manufacturer Aoshike, this PV cell should produce 0.46 watts under normal sunlight. The Experiment #2 model power output for 988 W/m^2 illumination flux was order-of-magnitude-comparable: 0.10 watts. However, the actual PV cell power output under this experimental condition was essentially nil (see Table 3). The PV cell was certainly connected as it did register power under 2450 W/m^2 illumination; albeit at a much lower level than anticipated. Poor PV power output in Experiment #2 might have arisen from a poor electrical connection between the apparatus PV cell and the electrical pickups, which were soldered manually to the cell's surface. Further testing is needed to ascertain the cause of this large and unexplained discrepancy.

At this generator size scale under concentrated illumination conditions ranging from 1X to 2.5X normal sunlight, the PV module should be producing more power than the TE, which is why design features that improve PV performance are expected to have greater impact on the overall system power output. Thus, adding forced convection, which has the dual effect of keeping the PV cooler relative to natural convection and driving more desirable heat transfer across the TE, induces better module performance than natural convection.

However, the resulting slight improvement in power output from forced convection comes at significant cost in parasitic power consumption from the fan driving the forced convection process. Even under the most favorable conditions examined using the analytical model, the largest output power increase owing to addition of forced convection is 50 mW. By comparison, creating that forced convection requires addition of a fan consuming at least 6.72 watts, which is greater than the whole PV/TE hybrid system's power output.

Recall the key research question of this paper. Is it better to actively cool or to passively cool hybrid PV/TE solar concentered generators at this size scale? The answer is passive cooling is better. A key conclusion from the model is that while forced convection does successfully keep the temperature of the PV/TE generator below the temperature induced from natural convection alone, the resulting minute power production increase does not justify use of an electric fan to force air over the TE cold end. Therefore, the best configuration for a solar concentrating PV/TE generator at this size scale is to rely on natural convection alone for TE cold side thermal management.

While not evaluated in this modeling process, the performance of the system could be improved by adding fins to the TE cold surface to increase surface area and further regulate temperature by passive cooling. Configurations with fins, both forced and natural convection, will be explored in the next iteration of the design process.

Modulating other solar collector and PV/TE module parameters, such as reflectivity, to increase the energy absorbed by the PV module reveals an inserting and unanticipated result. While T_{PV} increases under these conditions, reducing the PV module power output due to dropping solar cell efficiency, the resulting $T_{TE,hot}$ temperature increase induces larger power generation from the TE module. In fact, under forced convection at all $T_{PV} > 361$ K the power output of the TE module exceeds that of the PV module. Given that the TE was originally meant to merely supplement the PV as a bottoming cycle, this result is unexpected and suggests a different, TE-focused approach to design might be more effective: configuring the system to maximize $T_{TE,hot}$ under forced convection to regulate $T_{TE,cold}$.

CONCLUSIONS

A solar-concentrating hybrid PV/TE system was designed and built around a small upcycled television satellite dish following the *EELM*™ pedagogy. The goals of this system are 1) to maximize electrical power generation and 2) to provide a low-cost research and teaching tool enabling students to learn about solar-concentrating hybrid PV/TE technology. Design of this system, which occurred as part of a senior design Capstone experience, was supported by analytical modeling using a steady-state 1-dimensional model that considers either free or forced convection over the TE cold end. Two experimental apparatuses complementary to the model were built and run in an attempt to validate the model.

The concentrator used was a salvaged miniature satellite dish 19.33 inches long by 17.93 inches wide. It was coated with mirrored tape to reflect sunlight upon a focal point. Scavenged at no cost, the satellite dish is a sectioned paraboloid of rotation offset from the vertex and the axis of symmetry. However, which paraboloid section the dish represents is unknown. So, a technique is presented to find the focal point and to use this information to correctly position a shadow-casting gnomon to ensure proper on-sun alignment. A method to experimentally confirm the focal location and size the PV is also provided.

Two experimental apparatuses were built consisting of a PV module backed by TE generators and instrumented with thermocouples to determine the internal temperature gradient while multi-meters read steady-state PV and TE power output. A halogen lamp placed at various distances from this array approximates concentrated sunlight, which is measured via pyranometer. These experiments attempted to validate conclusions drawn from the theoretical model, but actual measured power outputs were significantly smaller than predicted by the analytical model or represented in manufacturer specification sheets. This anomaly remains unexplained.

To evaluate the fan power needed to induce forced convection over the TE cold end, experiments were conducted with an electrical drone fan to determine its start-up power threshold: 6.72 watts. Thus, to produce a net positive amount of power and provide value any forced convection system added to the PV/TE module must increase power output by at least 6.72 watts over the power produced when the module is cooled by natural convection. Given that the highest modeled and experimental outputs for the most powerful system studied were 1.023 watts and 0.49 watts respectively, it is never practical to add forced convection cooling to a hybrid PV/TE solar concentrating system at the size scale of an upcycled television satellite dish.

NOMENCLATURE

$A_{collector}$ = Aperture area of parabolic solar concentrator dish
A_{target} = Surface area of PV/TE module exposed to sunlight
D = Depth of parabolic satellite dish
$\dot{E}_{sun}$ = Solar flux rate [sun illumination ~1000 W/m^2]
F = Focal length
H = Height of parabolic satellite dish
h_{TE} = Convective heat transfer coefficient, TE external surface
h_{forced} = Convective heat transfer coefficient, forced convection
$h_{natural}$ = Convective heat transfer coefficient, natural convection
h_{PV} = Convective heat transfer coefficient, PV external surface
k_{PV} = Thermal conductivity for PV cell or PV module [W/m-K]
K_{TE} = Thermal conductance for TE generator [W/K]
L_{PV} = Thickness of PV cell or PV module
L_{TE} = Thickness of thermoelectric generator
$\dot{P}_{PV}$ = Electrical power produced by PV cell or module
$\dot{P}_{TE}$ = Electrical power produced by TE generator
$Q_{PV,out}$ = Rate of heat flux through a PV cell or module
T_{amb} = Ambient temperature
T_{PV} = PV face temperature at the center
$T_{PV,edge}$ = PV face temperature at the edge
$T_{PV,ref}$ = Ref. temp. [298 K] for PV efficiency model of Eq. 6
$T_{TE,cold}$ = TE cold face temperature
$T_{TE,hot}$ = TE hot face temperature
W = Width of parabolic satellite dish
Z = Thermoelectric figure of merit
α = Empirical PV cell efficiency for model of Eq. 6
β = Empirical PV cell thermal degradation coefficient for Eq. 6
η_{PV} = Photovoltaic cell efficiency
η_{TE} = Thermoelectric generator efficiency
Θ = Gnomon angle
$\rho_{collector}$ = Reflectivity, parabolic solar concentrator dish surface
ρ_{PV} = Reflectivity, photovoltaic cell surface

ACKNOWLEDGMENTS

We acknowledge in-kind donations of materials and volunteer time by Engineer Inc, a Florida-based engineering education technology company that established the principles and pedagogy of the Energy Engineering Laboratory Module, *EELM*™. Engineer Inc creates inexpensive teaching laboratory equipment for engineering courses: www.EngineerInc.net .

This paper's undergraduate authors are members of the Tennessee Undergraduate Researcher Network (TURN) at TSU, an organization that fast-tracks undergraduates into meaningful early research experiences. We also acknowledge Fletcher Henderickson of TURN who provided essential experimental data supporting the forced convection analysis. This project demonstrates the Undergraduate Researcher

Incubator Hypothesis [39,40], a corollary pedagogy within the Narrative of *New Learning* [41].

REFERENCES

[1] Grant, A. E., Meadows, J, H, Communication Technology Update, 10th ed., Focal Press, Inc., 2006, p. 87.

[2] Singh, T., "19-Year-Old Teenager Makes Homemade Solar Death Ray," Inhabitat.com, URL: http://inhabitat.com/19-year-old-teenager-makes-homemade-solar-death-ray/ , accessed 2/10/2017.

[3] Nuwayhid, R. Y., Mrad, F., Abu-Said, R., "The realization of a simple solar tracking concentrator for university research applications," *Renewable Energy*, Vol. 24, No. 2, 2001, pp. 207-222.

[4] Fallwell, C. M., Davis, D. W., Traum, M. J., "Solar Energy Concentration for Thermoelectric Power Generation at the Sub-Dekawatt Scale," AIAA Paper Number 2009-4246, *Proceedings of the 41st AIAA Thermophysics Conference*, San Antonio, TX, June 22 - 25, 2009.

[5] Xia, H., Luob, L., Fraisseb, G., "Development and applications of solar-based thermoelectric technologies," *Renewable and Sustainable Energy Reviews*, Vol. 11, 2007, pp. 923–936.

[6] Maneewan, S., Khedari, J., Zeghmati, B., Hirunlabh, J., Eakburanawat, J., "Investigation on generated power of thermoelectric roof solar collector," *Renewable Energy*, Vol. 29, 2004, pp. 743–752.

[7] Kraemer, D., Hu, L., Muto, A., Chen, X., Chen, G., Chiesa, M., "Photovoltaic-thermoelectric hybrid systems: A general optimization methodology," *Applied Physics Letters*, Vol. 92, 2008, pp. 243503-243506.

[8] Vorobiev, Y., Gonzalez-Hernandez, J., Vorobiev, P., Bulat, L., "Thermal-photovoltaic solar hybrid system for efficient solar energy conversion," *Solar Energy*, Vol. 80, 2006, pp. 170–176.

[9] Riffat, S. B., Ma, X., "Thermoelectrics: a review of present and potential applications," *Applied Thermal Engineering*, Vol. 23, 2003, pp. 913–935.

[10] Scherrera, H., Vikhorb, L., Lenoira, B., Dauschera, A., Poinasc, P., "Solar thermoelectric generator based on skutterudites," *Journal of Power Sources*, Vol. 115, 2003, pp. 141–148.

[11] Landis, G. A., Merritt, D., Raffaelle, R. P., Scheiman, D., "High-Temperature Solar Cell Development," *Proceedings of the 18th Space Photovoltaic Research and Technology Conference*, Brook Park, Ohio, September 16–18, 2003, pp. 241 – 247.

[12] Robert, R., Romer, S., Reller, A., Weidenkaff, A., "Nanostructured Complex Cobalt Oxides as Potential Materials for Solar Thermoelectric Power Generators," *Advanced Engineering Materials*, Vol. 7, No. 5, 2005, pp 303-308.

[13] Beeri, O., Rotem, O., Hazan, E., Katz, E. A. Braun, A., Gelbstein, Y, "Hybrid photovoltaic-thermoelectric system for concentrated solar energy conversion: Experimental realization and modeling," *Journal of Applied Physics*, Vol. 118, No. 11, 2015.

[14] Crisostomo, F., Taylor, R. A., Surjadi, D., Mojiri, A., Rosengarten, G., Hawkes, E. R., "Spectral splitting strategy and optical model for the development of a concentrating hybrid PV/T collector," *Applied Energy,* Vol. 141, 2015, pp. 238-246.

[15] Glynn, P., "More Heat than Light? Breakthrough solar cell harvests electricity from the sun's thermal energy," U.S. Department of Energy – Office of Science, 9/19/2011. https://science.energy.gov/news/featured-articles/2011/127021/

[16] Advanced Research Projects Agency - Energy (ARPA-E), "High-Temp, High-Efficiency Solar-Thermoelectric Generator Grant Program," U.S. Department of Energy, https://arpa-e.energy.gov/?q=slick-sheet-project/solar-thermoelectric-generator , Accessed 5/8/2017.

[17] DeWaters, J., Powers, S., "Work in progress - energy education and energy literacy: Benefits of rigor and relevance," *Proceedings of the 39th ASEE/IEEE Frontiers in Education Conference*, San Antonio, TX, 2009.

[18] Condoor, S., "Renewable Energy-Based Design Experience for Undergraduate Students," Paper AC 2011-1901, *Proceedings of the 118th ASEE Annual Conference & Exposition*, Vancouver, BC, Canada, June 26-29, 2011.

[19] Pantchenko, O. S., Tate, D. S., O'Leary, D., Isaacson, M. S., Shakouri, A., "Enhancing Student Learning Through Hands-On Laboratory Experiments on Renewable Energy Sources," *Paper AC 2011-75, Proceedings of the 118th ASEE Annual Conference & Exposition*, Vancouver, BC, Canada, June 26-29, 2011.

[20] Yang, Z., Weiss, H. L., Traum, M. J., "Gas Turbine Dynamic Dynamometry: A New Energy Engineering Laboratory Module," *Proceedings of the 2013 American Society for Engineering Education (ASEE) North Midwest Section Conference*, Fargo, North Dakota, October 17-18, 2013.

[21] Traum, M. J., Anderson, J. R., Pace, K., "An Inexpensive Inverted Downdraft Biomass Gasifier for Experimental Energy-Thermal-Fluids Demonstrations," *Proceedings of the 120th American Society for Engineering Education (ASEE) Conference and Exposition*, Atlanta, GA, June 23-26, 2013.

[22] Yang, Z., Weiss, H. L., Traum, M. J., "Dynamic Dynamometry to Characterize Disk Turbines for Space-Based Power," *Proceedings of the 23rd Annual Wisconsin Space Conference*, Milwaukee Wisconsin, August 15-16, 2013.

[23] Traum, M. J., "Harvesting Built Environments for Accessible Energy Audit Training," *Proceedings of the 2nd International Conference on the Constructed Environment*, Chicago, IL, October 29-30, 2011.

[24] Cross, N., Roy, R., Engineering Design Methods, 4th Ed., Wiley, New York, NY, 2008.

[25] Hadi, F., Akbar, M. K., Traum, M. J., "Applying Trigonometry to a Pervasive Solar Energy Engineering Problem," *International Journal of Mechanical Engineering Education*, in preparation.

[26] Skoplaki, E., Palyvos, J. A., "On the temperature dependence of photovoltaic module electrical performance: A review of efficiency/power correlations," *Solar Energy*, Vol. 83, 2009, pp. 614–624.

[27] Furushima, K., Nawata, Y., "Performance Evaluation of Photovoltaic Power-Generation System Equipped With a Cooling Device Utilizing Siphonage," *Journal of Solar Energy Engineering*, Vol. 128, No. 2, 2006, pp. 146-151.
[28] Mills, A. F., Heat Transfer, 2nd Edition, Prentice Hall, Upper Saddle River, NJ, 1999, p. 22.
[29] Honsberg C, Bowden, S., "General Properties of Silicon," PV Education Web site, http://pveducation.org/pvcdrom/materials/general-properties-of-silicon , accessed 8/7/2017.
[30] Goupil, C., Seifert, W., Zabrocki, K., Müller, E., Snyder, G. J., "Thermodynamics of thermoelectric phenomena and applications," *Entropy*, Vol. 13, No. 8, 2011, pp. 1481-1517.
[31] Luo, Z., "A Simple Method to Estimate the Physical Characteristics of a Thermoelectric Cooler from Vendor Datasheets," *Electronics Cooling Magazine*, Vol. 14, No. 3, 2008, pp. 22-27.
[32] Hebei I.T. (Shanghai) Co., Ltd, "TEC1-12730 Thermoelectric Cooler Specification Sheet," URL: http://www.hebeiltd.com.cn/peltier.datasheet/TEC1-12730.pdf , accessed 8/7/2017.
[33] Baranowski, L. L., Snyder, G. J., Toberer, E. S., "Concentrated solar thermoelectric generators," *Energy & Environmental Science*, Vol. 5, No. 10, 2012, pp. 9055-9067.
[34] Barlve, D., Vidu, R., Stroeve, P., "Innovation in concentrated solar power," *Solar Energy Materials and Solar Cells*, Vol. 95, No. 10, 2011, pp. 2703-2725.
[35] Kemmoku, Y., Egami, T., Hiramatsu, M., Miyazaki, Y., Araki, K., Ekins-Daukes, N. J., Sakakibara, T., "Modeling of Module Temperature of a Concentrator PV System," *Proceedings of the 19th European Photovoltaic Solar Energy Conference and Exhibition*, Paris, France, 2004, pp. 2568-2672.
[36] Notton, G., Cristofari, C., Mattei, M., Poggi, P., "Modeling of a double-glass photovoltaic module using finite differences," *Applied Thermal Engineering*, Vol. 25, 2005, pp. 2854–2877.
[37] Quaschning, V., Understanding Renewable Energy Systems, 2nd Edition, Earthscan Publications, Ltd., New York, NY, 2005, Page 138.
[38] Traum, M. J., Griffith, P., Thomas, E. L., Peters, W. A., "Latent Heat Fluxes Through Soft Materials With Micro-truss Architectures," *ASME Journal of Heat Transfer*, Vol. 130, April 2008, pp. 042403-1 to 042403-11.
[39] Traum, M. J., Karackattu, S. L., Houston Jackson, D., McNutt, J. D., "Organization to Fast-Track Undergraduate Students Into Engineering Research via Just-In-Time Learning," *Proceedings of the Conference On Being an Engineer: Cognitive Underpinnings of Engineering Education*, Lubbock, TX, February 1-2, 2008.
[40] Traum, M. J., Karackattu, S. L., "The Researcher Incubator: Fast-tracking Undergraduate Engineering Students into Research via Just-in-Time Learning," ASEE GSW Paper Number 09-33, *Proceedings of the 2009 ASEE Gulf-Southwestern Section Annual Conference*, Waco, TX, March 18 – 20, 2009.
[41] Kalantzis, M., Cope, B., New Learning: Elements of a Science Education, 2nd Edition, Cambridge University Press, New York, NY, 2012.